

## Supporting Information

### Probing the role of surface acidity on photocatalytic degradation of tetracycline hydrochloride over cerium doped CdS via experiments and theoretical calculations

Ran Chen <sup>a, b, †</sup>, Juan Chen <sup>a, †</sup>, Xin Gao <sup>a</sup>, Yanhui Ao <sup>a, \*</sup>, Peifang Wang <sup>a</sup>

<sup>a</sup> Key Laboratory of Integrated Regulation and Resource Development on Shallow Lakes, Ministry of Education, College of Environment, Hohai University, No.1, Xikang road, Nanjing, 210098, China

<sup>b</sup> College of Life & Environmental Sciences, Huangshan University, Huangshan, 245041, China

#### Characterization

The structure of all the catalyst were analyzed by employing X-ray diffraction (XRD) characterization through using Shimadzu/XD-3A instrument (Cu K $\alpha$  radiation). The datum was gathered at a 2 $\theta$  range of 10-80°. Transmission electron microscopy (TEM) was characterized by a FEI TECNAI G20 system. scanning electron microscope (SEM) was carried out via a HITACHI S-4800 equipment. ESR was employed by a Jes FA 200 equipment. UV-vis diffuse reflectance spectra (DRS) was measured by a Shimadzu/UV-3600. Photoluminescence (PL) analysis was employed on a Hitachi/F-7000 system. X-ray photoelectron spectra (XPS) was then employed by using a Thermo Scientific ESCALAB 250 equipment with Al-K $\alpha$  radiation. Temperature programmed desorption of NH<sub>3</sub> (NH<sub>3</sub>-TPD) was carried out by an AutoChemi 2920 equipment. Pyridine adsorbed IR spectroscopy (Py-IR) was adopted on a Thermo Nicolet 380 instrument. Inductively coupled plasma (ICP) was

---

\* Corresponding author. E-mail address: [andyao@hhu.edu.cn](mailto:andyao@hhu.edu.cn) (Yanhui Ao)

employed by an Agilent ICPMS 7700 equipment. Electrochemical property of all the samples was acquired in 0.5M H<sub>2</sub>SO<sub>4</sub> by using a typical three electrode setup on an electrochemical station (Chenhua Instruments, CHI660D) with an Ag/AgCl reference electrode, Pt foil as counter electrode and CdS composites as working electrode.

### Density functional theory (DFT) calculation analysis

Fukui function based on the density functional theory (DFT) was used to predict the regioselectivity of ROS ( $\cdot\text{O}_2^-$ ) towards the TC molecules. All of the calculations were performed using the Gaussian 16 (Revision C.01) software [1]. The geometry optimization and single-point energy calculations were executed using the B3LYP method with the 6-31G\* basis set. Fukui function is an important concept in the conceptual density functional theory (CDFT), and it has been widely used in prediction of reactive sites of electrophilic, nucleophilic and general radical attacks [2]. Specifically, Fukui function is defined as:

$$f(\mathbf{r}) = \left[ \frac{\partial \rho(\mathbf{r})}{\partial N} \right]_v$$

(1)

where  $\rho(\mathbf{r})$  is the electron density at a point  $\mathbf{r}$  in space,  $N$  is the electron number in the present system, and the constant term  $v$  in the partial derivative is the external potential. In the condensed version of Fukui function, the atomic population number is used to represent the electron density distribution around an atom. The condensed Fukui function can be calculated as:

Electrophilic attack:  $f_A^- = q_{N-1}^A - q_N^A$

(2)

Nucleophilic attack:  $f_A^+ = q_N^A - q_{N+1}^A$

(3)

Radical attack:

$$f_A^0 = (q_{N-1}^A - q_{N+1}^A)/2$$

(4)

Condensed dual descriptor:  $\Delta f_A = f_A^+ - f_A^-$  (5)

where  $q^A$  is the atom charge of atom A at the corresponding state.

### **Photocatalytic performance**

In a typical experiment, 25 mg photocatalyst was dispersed in 100 mL of 10 mg/L TC-HCl aqueous solution. Before irradiation, the above suspension was stirred in the dark for 60 min to reach the adsorption-desorption equilibrium. Then the suspension was illuminated under visible light, sampled at regular intervals of 1 min and centrifuged to remove the catalyst at 10000 rpm for 3 min. The concentration of TC-HCl solution was detected by a high-performance liquid chromatograph (HPLC, Waters e2695). The initial concentration ( $C_0$ ) was considered to be the TC-HCl concentration after adsorption-desorption equilibrium.

**For the reusability tests, 25 mg of as prepared 5% Ce-CdS samples were dispersed in 100 mL of 10 mg/L TC-HCl aqueous solution. Before irradiation, the above suspension was stirred in the dark for 60 min to reach the adsorption-desorption equilibrium. Then the solution was illuminated under visible light, sampled at regular intervals of 1 min. Recycle the catalysts after finished the photocatalytic tests by centrifuging at 10000 rpm and dried in oven at 60 °C for 12h. Repeat the procedures to finish the reusability tests.**

**For the adsorption process, 25 mg of as prepared x% Ce-CdS samples were dispersed in 100 mL of 10 mg/L TC-HCl aqueous solution at dark condition for 60 min. Collect the TC-HCl solution at different times. Centrifuge the solution to remove the catalyst at 10000 rpm for 3 min. The concentration of TC-HCl solution was detected by a high-performance liquid chromatograph.**

Photocatalytic performance of H<sub>2</sub> generation was carried out in a 100 mL quartz reactor that suffused with 50 mL DI water. Then, 5 mg catalysts were added in water together with 0.25 M sodium sulfide and 0.35 M sodium sulfite and kept stirring for several minutes. Next, degas the circulation system in order to keep the system vacuumed. After that, turn on the 300 W xenon lamp with a 420 nm cut-off filter as the light source (CELHXF300, Beijing China Education Au-light Co., Ltd). At last, the produced H<sub>2</sub> was analyzed by an online gas chromatogram (GC 7900) equipped with a thermal conductivity detector.

Figure S1 NH<sub>3</sub>-TPD results of 1% Ce-CdS and 10% Ce-CdS.

Figure S2 (a-b) Py-IR results of 1% Ce-CdS and 10% Ce-CdS.

Figure S3 Low and high magnification of SEM images of CdS (a-b) and 5% Ce-CdS samples (c-d).

Figure S4 Recycling photocatalytic degradation of TC-HCl over 5% Ce-CdS.

Fig. S5 XPS results of 5% Ce-CdS photocatalysts after 3 runs, high-resolution signals of S 2p (a); Cd 3d (b) and Ce 3d (c)

Figure S6 The effects of anions (5 mM) on TC-HCl photodegradation.

Figure S7 The effects of humic acids on TC-HCl photodegradation.

Figure S8 The effects of pollutants concentration on TC-HCl photodegradation.

Figure S9 Hydrogen production rate of CdS and 5% Ce-CdS samples.

Figure S10 Mott-schottky characterization of CdS and x% Ce-CdS samples.

Table S1 Comparison of photodegradation of TC over CdS-based catalysts.

Table S2 HPLC-MS data for the intermediate products during TC-HCl degradation.

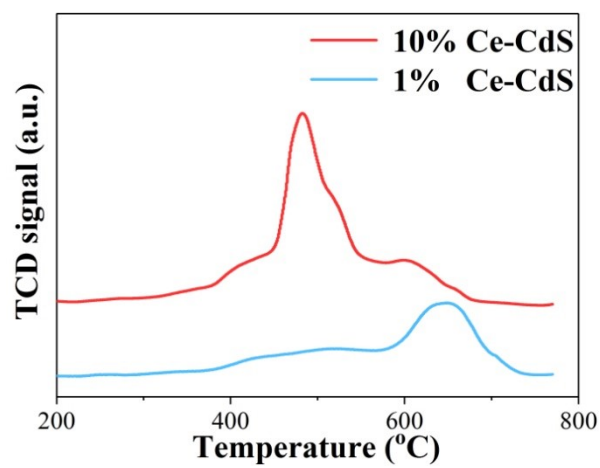


Figure S1 NH<sub>3</sub>-TPD results of 1% Ce-CdS and 10% Ce-CdS.

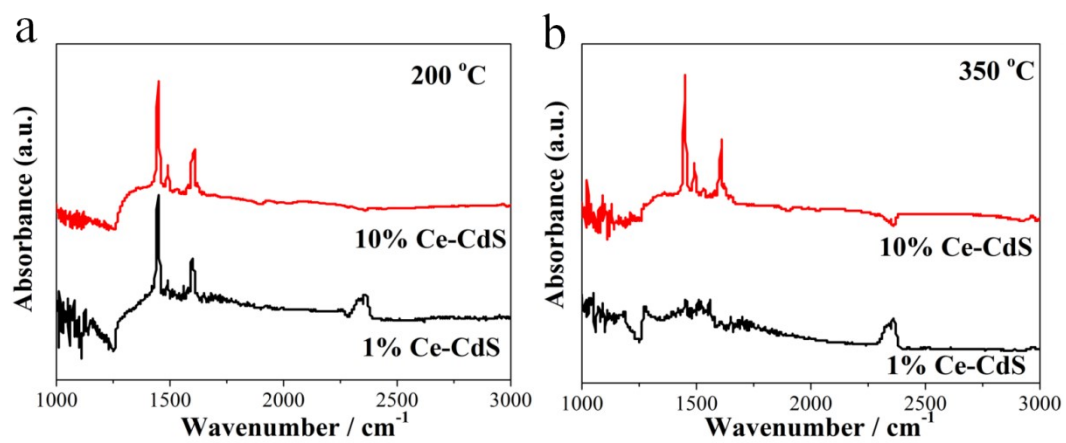


Figure S2 (a-b) Py-IR results of 1% Ce-CdS and 10% Ce-CdS.

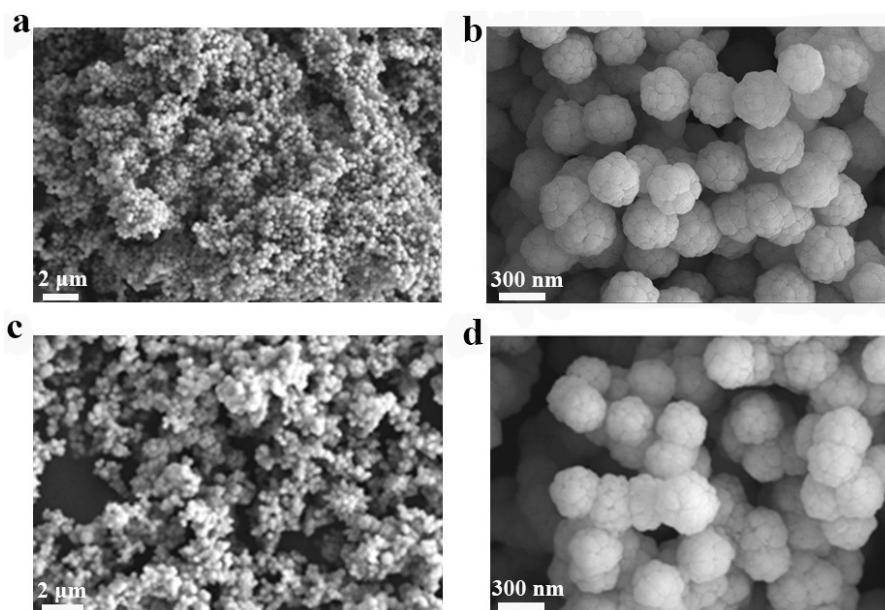


Figure S3 Low and high magnification of SEM images of CdS (a-b) and 5% Ce-CdS samples (c-d).

SEM images of CdS and 5% Ce-CdS photocatalysts with low and high magnification are shown in Fig. S3. Clearly, 5% Ce-CdS keep similar shape with CdS, testifying the addition of Ce has no effect on the morphology of CdS.



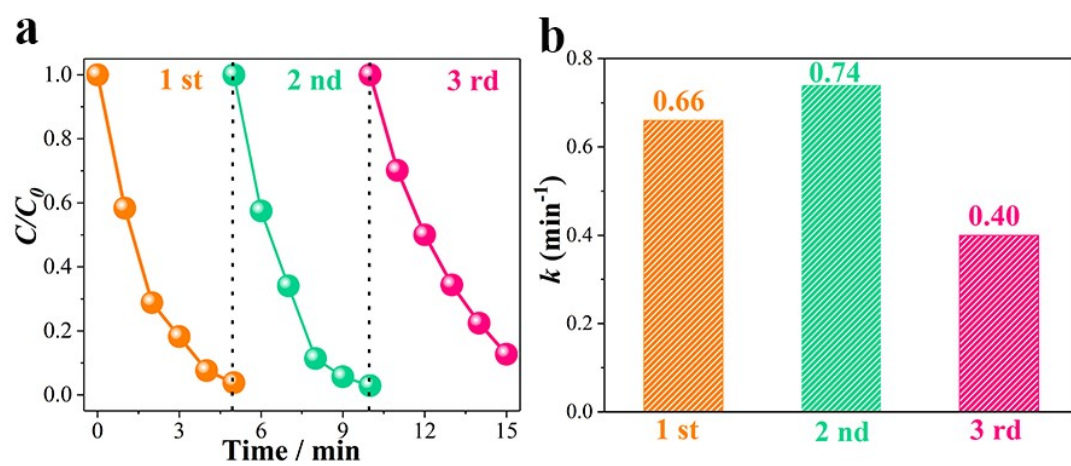


Figure S4 Recycling photocatalytic degradation of TC-HCl over 5% Ce-CdS.

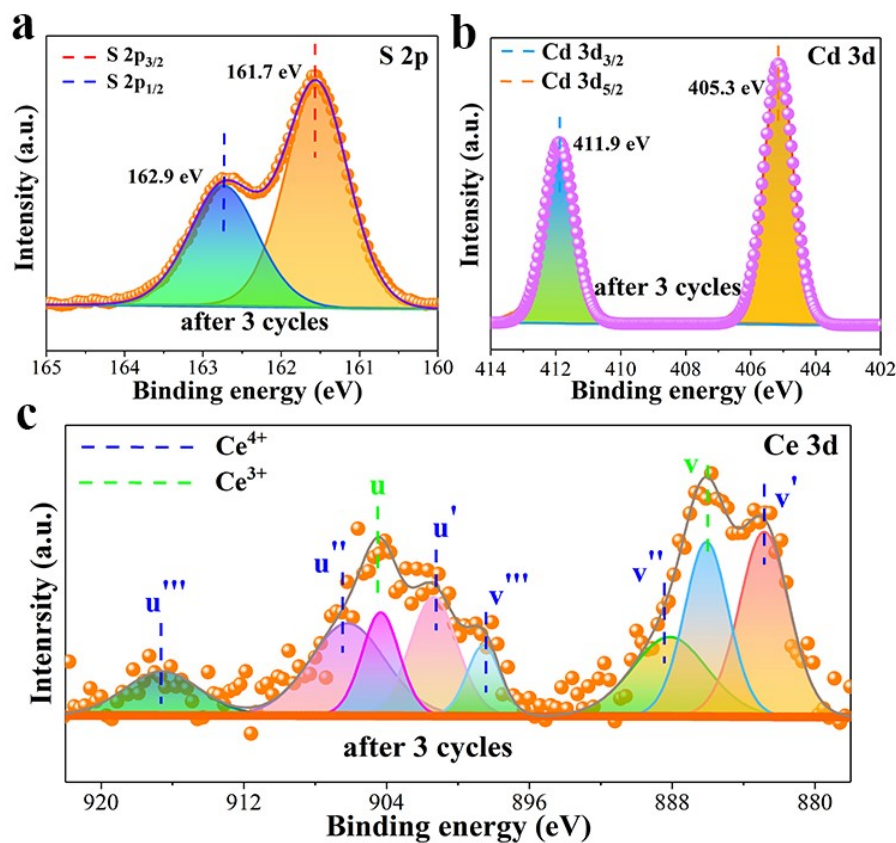


Fig. S5 XPS results of 5% Ce-CdS photocatalysts after 3 runs, high-resolution signals of S 2p (a); Cd 3d (b) and Ce 3d (c)

$Ce^{3+}/Ce^{4+}$  results before and after 3 cycles based on XPS characterizations was calculated to be 0.28 and 0.35, respectively. In our work, polarization effect of Ce ions with water molecules makes the hydrogen ions formed and thus become Brönsted acid sites<sup>[3]</sup>. It is proved that Brönsted acid sites favor the adsorption of organic molecules. Part of  $Ce^{4+}$  will be converted to  $Ce^{3+}$  during the photocatalytic process. Thereafter, the catalysts will be deactivated (Fig. S4) and less pollutants could be adsorbed on the catalyst, leading to a reduced photocatalytic performance.

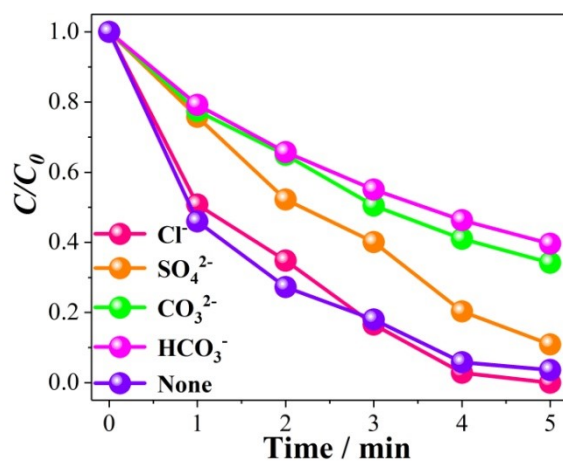


Figure S6 The effects of anions (5 mM) on TC-HCl photodegradation.

Considering the complexity of water environment, photocatalytic degradation efficiency will be changed in practice. Different anions ( $\text{Cl}^-$ ,  $\text{SO}_4^{2-}$ ,  $\text{HCO}_3^-$  and  $\text{CO}_3^{2-}$ ) were added into the solution that contained catalysts and pollutants to evaluate the photodegradation efficiency of TC-HCl. In Fig. S6,  $\text{Cl}^-$  had nearly no effect on the degradation efficiency while  $\text{SO}_4^{2-}$  could partially affect the performance. For  $\text{HCO}_3^-$  and  $\text{CO}_3^{2-}$ , photocatalytic activity will be suppressed significantly. The existence of Coulombic repulsion between TC-HCl molecules, photocatalysts,  $\text{HCO}_3^-$  and  $\text{CO}_3^{2-}$  is mainly responsible for the reduced photocatalytic performance<sup>[4]</sup>.

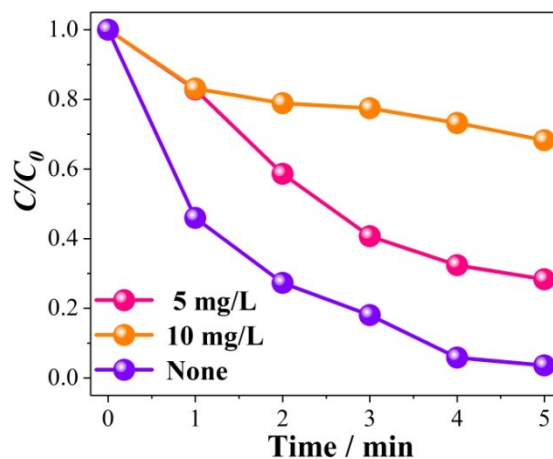


Figure S7 The effects of humic acids on TC-HCl photodegradation.

Humic acid is a kind of significant constituent in water environment, which could hinder degradation performance (Fig. S7)<sup>[5]</sup>. Explicitly, photocatalytic activity for TC-HCl degradation shows gradual restriction with the increasing concentration of humic acid. The addition of humic acid will consume reactive oxygen species. Moreover, humic acid may shield the absorption of visible light<sup>[6]</sup>.

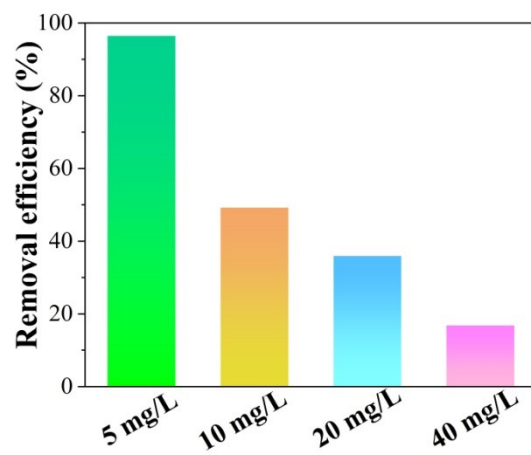


Figure S8 The effects of pollutants concentration on TC-HCl photodegradation.

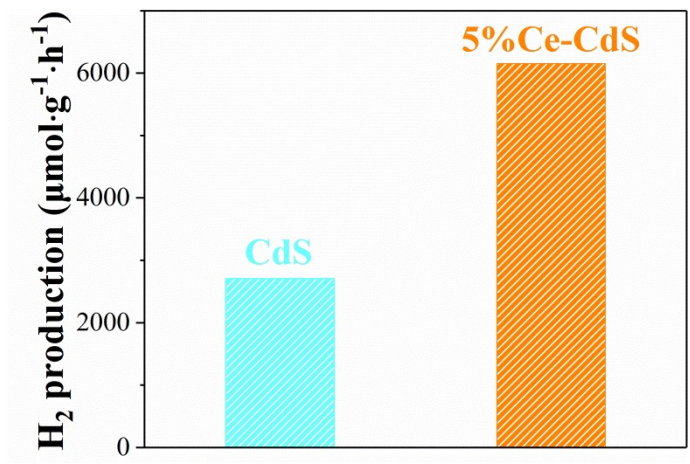


Figure S9 Hydrogen production rate of CdS and 5% Ce-CdS samples.

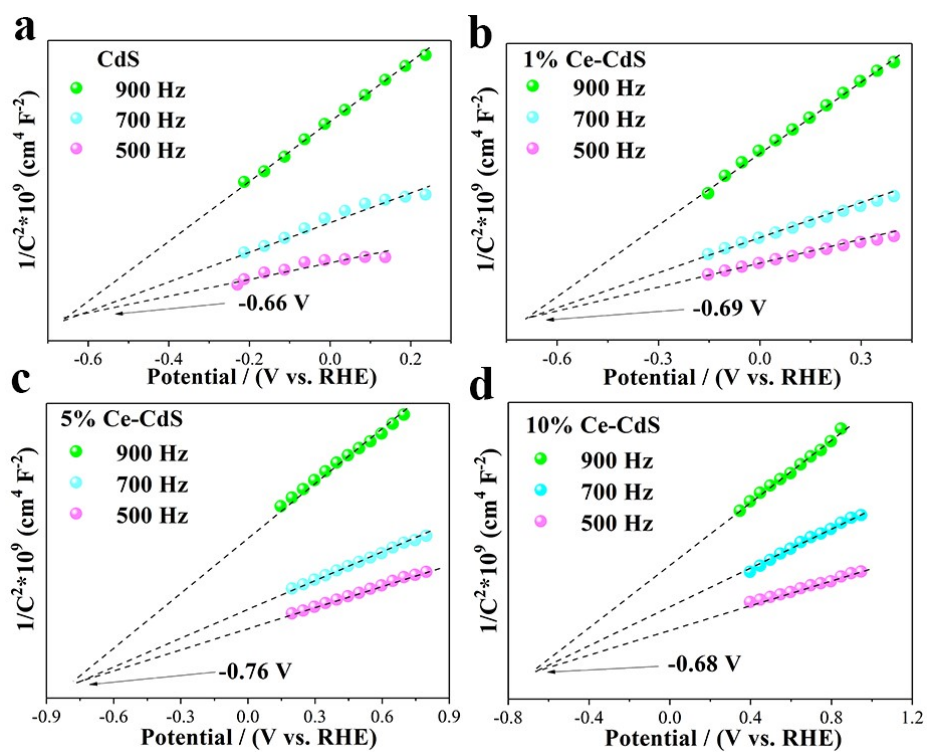


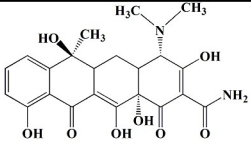
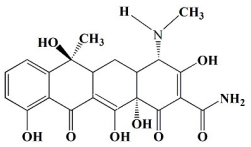
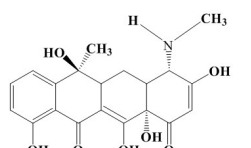
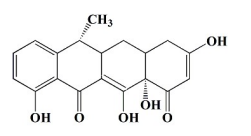
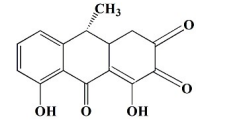
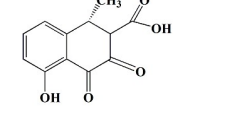
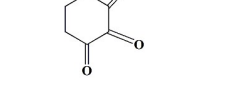
Figure S10 Mott-schottky characterization of CdS and x% Ce-CdS samples.

Table S1 Comparison of photodegradation of TC over CdS-based catalysts.

Photocatalysts	Concentration of TC (ppm)	Light source	Degradation of TC in 5 min (%)	Irradiated time (min)	Ref.
CdS-ZIF-8-C	30	Visible	100	60	7
CF/C <sub>3</sub> N <sub>4</sub> /CdS	20	Visible	81	60	8
CdS/NiCo <sub>2</sub> O <sub>4</sub>	25	Visible	~80	90	9
BOI-CBBMO	20	Visible	87	60	10
GO/PAA-CdS	30	Visible	86	240	11
BiVO <sub>4</sub> -CdS	20	Visible	82.1	25	12
CdS/HAP	50	Visible	90.2	30	13
CdS@CeO <sub>2</sub>	50	Visible	91.5	60	14
CdS-TiO <sub>2</sub>	50	Visible	87.06	480	15
<b>Ce-CdS</b>	<b>10</b>	<b>Visible</b>	<b>95.9</b>	<b>5</b>	<b>This work</b>



Table S2 HPLC-MS data for the intermediate products during TC-HCl degradation.

Compounds	m/z	Molecular formula	Possible structure	Retention Time/min
P1	445	C <sub>22</sub> H <sub>22</sub> O <sub>8</sub> N <sub>2</sub>		2.18
P2	431	C <sub>21</sub> H <sub>23</sub> O <sub>8</sub> N <sub>2</sub>		0.12
P3	388	C <sub>20</sub> H <sub>22</sub> O <sub>7</sub> N		2.66
P4	343	C <sub>19</sub> H <sub>19</sub> O <sub>6</sub>		2.25
P5	271	C <sub>15</sub> H <sub>11</sub> O <sub>5</sub>		0.54
P6	232	C <sub>12</sub> H <sub>8</sub> O <sub>5</sub>		0.71
P7	123	C <sub>6</sub> H <sub>3</sub> O <sub>3</sub>		2.87

- [1] M. J. Frisch, G. W. Trucks, H. B. Schlegel, G. E. Scuseria, M. A. Robb, J. R. Cheeseman, G. Scalmani, V. Barone, G. A. Petersson, H. Nakatsuji, Li, M. Caricato, A. V. Marenich, J. Bloino, B. G. Janesko, R. Gomperts, B. Mennucci, H. P. Hratchian, J. V. Ortiz, A. F. Izmaylov, J. L. Sonnenberg, D. Williams-Young, F. Ding, F. Lipparini, F. Egidi, J. Goings, B. Peng, A. Petrone, T. Henderson, D. Ranasinghe, V. G. Zakrzewski, J. Gao, N. Rega, G. Zheng, W. Liang, M. Ehara, K. Toyota, R. Fukuda, J. Hasegawa, M. Ishida, T. Nakajima, Y. Honda, O. Kitao, H. Nakai, T. Vreven, K. Throssell, J. A. Montgomery, Jr., J. E. Peralta, F. Ogliaro, M. J. Bearpark, J. J. Heyd, E. N. Brothers, K. N. Kudin, V. N. Staroverov, T. A. Keith, R. Kobayashi, J. Normand, K. Raghavachari, A. P. Rendell, J. C. Burant, S. S. Iyengar, J. Tomasi, M. Cossi, J. M. Millam, M. Klene, C. Adamo, R. Cammi, J. W. Ochterski, R. L. Martin, K. Morokuma, O. Farkas, J. B. Foresman, and D. J. Fox, Gaussian, Inc., Wallingford CT, 2019.
- [2] R. G. Parr, W. T. Yang, Density functional-approach to the frontier-electron theory of chemical-reactivity, *J. Am. Chem. Soc.* 106 (1984) 4049-4050.
- [3] B. Thomas, S. Prathapan, S. Sugunan, Beckmann rearrangement of E, E-cinnamaldoxime on rare earth exchanged ( $Ce^{3+}$ ,  $La^{3+}$ , and  $RE^{3+}$ ) HFAU-Y zeolites: An efficient green process for the synthesis of isoquinoline. *Micropor. Mesopor. Mat.*, 84 (2005) 137-143.
- [4] R. Jiang, G. Lu, Z. Yan, D. Wu, R. Zhou, X. Bao, Insights into a CQD-SnNb<sub>2</sub>O<sub>6</sub>/BiOCl Z-scheme system for the degradation of benzocaine: Influence factors, intermediate toxicity and photocatalytic mechanism, *Chem. Eng. J.*, 374 (2019) 79-90.
- [5] D. Vione, V. Maurino, C. Minero, M.E. Carlotti, S. Chiron, S. Barbati, Modelling

the occurrence and reactivity of the carbonate radical in surface freshwater, *C.R. Chim.*, 12 (2009) 865-871.

[6] J. Liu, C. Li, R. Qu, L. Wang, J. Feng, Z. Wang, Kinetics and mechanism insights into the photodegradation of hydroperfluorocarboxylic acids in aqueous solution, *Chem. Eng. J.*, 348 (2018) 644-652.

[7] S. Y. Liu, Y. Ning, X. R. Qi, J. J. Zhao, Y. F. Fu, B. Y. Zhang, J. Gao, J. R. Miao, J. Z. Song, Q. Huo, CdS-modified ZIF-8-derived porous carbon for organic pollutant degradations under visible-light irradiation, *Res. Chem. Intermediate.*, DOI: 10.1007/s11164-021-04520-9.

[8] X. F. Shen, Y. Zhang, Z. Shi, S. D. Shan, J. S. Liu, L. S. Zhang, Construction of C<sub>3</sub>N<sub>4</sub>/CdS nanojunctions on carbon fiber cloth as a filter-membrane-shaped photocatalyst for degrading flowing wastewater, *J. Alloy Compd.*, 851 (2021) 156743.

[9] D. C. Hu, Y. Y. Xu, S. Y. Zhang, J. B. Tu, M. Li, L. H. Zhi, J. C. Liu, Fabrication of redox-mediator-free Z-scheme CdS/NiCo<sub>2</sub>O<sub>4</sub> photocatalysts with enhanced visible-light driven photocatalytic activity in Cr(VI) reduction and antibiotics degradation, *Collid. Surface A*, 608 (2021) 125582.

[10] D. Kandi, A. Behera, S. Sahoo, K. Parida, CdS QDs modified BiOI/Bi<sub>2</sub>MoO<sub>6</sub> nanocomposite for degradation of quinolone and tetracycline types of antibiotics towards environmental remediation, *Sep. Purif. Technol.*, 253 (2020) 117523.

[11] W. J. Kong, Y. Gao, Q. Y. Yue, Q. Li, B. Y. Gao, Y. Kong, X. D. Wang, P. Zhang, Y. Wang, Performance optimization of CdS precipitated graphene oxide/polyacrylic acid composite for efficient photodegradation of chlortetracycline, *J. Hazard. Mater.*, 388 (2020) 121780.

[12] Z. S. Wu, Y. T. Xue, X. F. He, Y. F. Li, Z. L. Wu, G. Cravotto, Surfactants-assisted preparation of BiVO<sub>4</sub> with novel morphologies via microwave method and CdS decoration for enhanced photocatalytic properties, *J. Hazard. Mater.*, 387 (2020) 122019.

[13] X. F. Lei, T. H. Xu, W. F. Yao, Q. Wu, R. J. Zou, Hollow hydroxyapatite microspheres modified by CdS nanoparticles for efficiently photocatalytic

degradation of tetracycline, J. Taiwan Inst. Chem. E., 106 (2020) 148-158.

[14] J. Xu, M. Li, J. H. Qiu, X. F. Zhang, Y. Feng, J. F. Yao, PEGylated deep eutectic solvent-assisted synthesis of CdS@CeO<sub>2</sub> composites with enhanced visible light photocatalytic ability, Chem. Eng. J., 383 (2020) 123135.

[15] W. Li, H. Ding, H. Ji, W. B. Dai, J. P. Guo, G. X. Du, Photocatalytic degradation of Tetracycline hydrochloride via a CdS-TiO<sub>2</sub> heterostructure composite under visible light irradiation, Nanomaterials, 8 (2018) 415.